

Magnetic anisotropy and interlayer exchange coupling of evaporated Au/Co multilayers

Peng Chubing, Dai Daosheng, and Fang Ruiyi

Department of Physics, Peking University, Beijing 100871, People's Republic of China

(Received 12 September 1991; revised manuscript received 23 March 1992)

The magnetic properties of Au/Co multilayers, prepared by the *e*-beam evaporation method, have been systematically studied by magnetic measurements and ferromagnetic resonance (FMR). In FMR spectra with the static magnetic field parallel to the film plane, a main mode and a higher-field mode have been identified, and understood as a result of the difference of outermost Co layers from internal Co layers. The interface-induced anisotropy has been revealed by both magnetic measurements and FMR spectra. Furthermore, the strong dependence of the magnetic properties, including the ratio of remanence to saturation magnetization and coercivity which characterize hysteresis loops, on the thicknesses of Au layers has been observed and is attributed to the effect of interlayer exchange coupling.

INTRODUCTION

The rich magnetic properties of artificial magnetic multilayers and ultrathin ferromagnetic films have been extensively studied in recent years. Very large perpendicular magnetic anisotropy exists in some of these thin-film systems and is particularly interesting from a fundamental point of view as well as for their potential application to recording media.¹ The magnetic anisotropy may be caused by various mechanisms, including shape anisotropy, magnetocrystalline anisotropy, magnetostriction, or the reduced symmetry at interfaces. The interface-induced anisotropy is strongly dependent on preparation techniques and conditions. By postannealing, the uniaxial anisotropy of Au/Co multilayers prepared by ion-beam sputtering was enhanced, leading to the easy magnetization direction normal to the film plane for a thickness of the Co layer less than 10 Å.² Moreover, research on interlayer exchange coupling of magnetic multilayers and double layers is becoming active, and many characteristic of interlayer coupling have been discovered, such as anti-ferromagnetic, ferromagnetic, and oscillating exchange couplings.^{3,4}

In this work we have primarily investigated the magnetic anisotropy and interlayer exchange coupling of Au/Co multilayers by magnetic measurements and by the ferromagnetic resonance (FMR) method. FMR studies are particularly suitable for providing information on magnetic anisotropy of thin film,⁵ and are a possible method for obtaining information on interlayer coupling.^{6,7} In the FMR spectra of our Au/Co multilayers, a higher-field mode besides a main mode was observed. The interface anisotropy is discussed in detail from magnetic measurements and FMR. Moreover, the strong dependence of the ratio of remanence to saturation magnetization and coercivity in hysteresis loops on thickness of Au layers was obtained, and is attributed to the effect of interlayer magnetic coupling.

EXPERIMENTS

Au/Co multilayers were prepared by using electron-beam deposition under vacuum 3×10^{-7} Torr. The depo-

sition process was computer controlled so that the motor-driven materials holder was turned to target position successively, and the deposition could be interrupted for materials positioning to ensure a good reproducibility and normally rectangular chemical composition profiles. Deposition rates of order 1 Å/s were monitored by a water-cooled quartz crystal oscillator. A float glass was used for the substrate. Prior to deposition, the substrates were cleaned in vacuum by heating to 250°C for half an hour in order to drive off impurities on the surface. Then the substrates were cooled to 70°C, Au/Co multilayers with Au layer thicknesses ranging from 5 to 30 Å and Co layer thicknesses of 10–40 Å were made. The total thickness of the film was about 800 Å.

X-ray-diffraction (XRD) data were taken on a standard θ - 2θ diffractometer using Cu K_α radiation in a geometry with the scattering vector normal to the film plane. Magnetic properties were evaluated using a vibrating sample magnetometer (VSM) with the magnetic field parallel and perpendicular to the film plane at room temperature. In addition, FMR measurements on Au/Co multilayers were carried out with a high-sensitivity electron paramagnetic resonance (EPR) spectrometer working at the X band (9.8 GHz). The FMR spectra were investigated as a function of an orientation of the applied dc field H in a plane perpendicular to the film plane at room temperature. The signal detected corresponds to the field derivative of the absorbed power.

RESULTS AND DISCUSSIONS

Figure 1 shows the typical low-angle and large-angle XRD patterns. At least three Bragg diffraction peaks are observed in low-angle XRD, confirming that the evaporated Au/Co multilayers exhibit periodic layered structure. In large-angle XRD profiles, superlattice peaks around the Au(111) reflection are observed to third order indicative of a high degree of order and good control of the fabrication process. Moreover, the position of the Au(111) peak is located between that of the fcc (111) of pure Au metal and hcp Co(00.2) reflections, and depends on the relative amount of Au and Co layers due to a mismatch of Au and Co lattice spacings. The absence

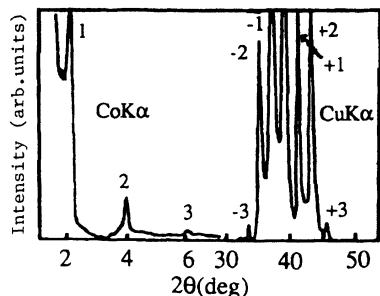


FIG. 1. X-ray-diffraction pattern of a $[\text{Au}(20 \text{ \AA})/\text{Co}(30 \text{ \AA})]_{20}$ multilayer.

of a Au fcc (200) reflection peak in the large-angle XRD profiles shows that the Au layer has pronounced (111) texture. The modulation period deduced from the position of the Bragg peaks in low-angle XRD and recalibrated by relative position of superlattice peaks in large-angle XRD is in agreement with the nominal value within 5%.

Figure 2 displays the hysteresis loops $M(H)$ at room temperature for $[\text{Au}(20 \text{ \AA})/\text{Co}(10 \text{ \AA})]_{27}$ and $[\text{Au}(20 \text{ \AA})/\text{Co}(30 \text{ \AA})]_{25}$ multilayers. It is seen that the magnetic moment is more easily magnetized to saturation in parallel geometry than in perpendicular geometry for $t_{\text{Co}} > 10 \text{ \AA}$, but that the easy magnetization direction of Au/Co multilayers moves out of the film plane when $t_{\text{Co}} < 10 \text{ \AA}$.⁸

In order to estimate the interface anisotropy K_s , the total magnetic anisotropy K_u per Co volume is divided into two parts:

$$K_u = K_v + 2K_s/t_{\text{Co}} \quad (1)$$

where K_v is bulk magnetic crystalline anisotropy. K_u , from which the shape anisotropy energy ($-2\pi\sigma_s^2$) has been extracted, is determined from hysteresis loops. The experimental data have been fitted using Eq. (1), and yield $K_v = 4 \times 10^6 \text{ erg/cm}^3$ and $K_s = 0.17 \text{ erg/cm}^2$, as shown in Fig. 3. The K_s value might be compared with 0.15 erg/cm^2 for evaporated Co/Cu multilayers,⁹ but it is less than that for the annealed Co/Au multilayers,² It seems that the interface-induced anisotropy may be strongly influenced by interface roughness as expected theoretically.¹⁰

Figure 4 shows the dependence of σ_r/σ_s (remnance to saturation magnetization) and H_c (coercivity) on a thickness of a Au layer (t_{Au}) for Au/Co multilayers with a fixed Co layer thickness of 10 \AA in magnetic field parallel to the film plane. It is seen that both σ_r/σ_s and H_c

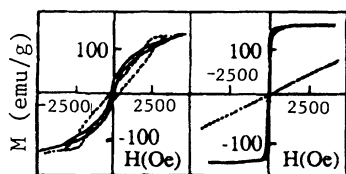


FIG. 2. Hysteresis loops for (a) $[\text{Au}(20 \text{ \AA})/\text{Co}(10 \text{ \AA})]_{27}$ and (b) $[\text{Au}(20 \text{ \AA})/\text{Co}(30 \text{ \AA})]_{25}$ multilayers in fields parallel (solid line) and perpendicular (dotted line) to the film plane.

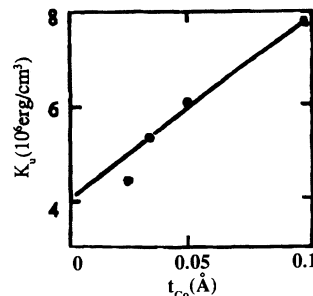


FIG. 3. A plot of magnetic anisotropy K_u as a function of $1/t_{\text{Co}}$ for multilayers with a fixed Au layer thickness of 30 \AA .

decrease rapidly with the increase of t_{Au} for t_{Au} up to 15 \AA , and approach constant when $t_{\text{Au}} > 15 \text{ \AA}$. These characteristics may be understood by interlayer magnetic coupling. It was theoretically calculated that Fe-Fe interlayer coupling for Fe/Au/Fe double layers is ferromagnetic, and that the strength of the coupling decreases rapidly with the increase of Au layer thickness when $t_{\text{Au}} < 15 \text{ \AA}$.³ The characteristics of interlayer coupling in an Fe/Au/Fe sandwich may be suitable to explain the behaviors of H_c and σ_r/σ_s in our Au/Co multilayers. Since neighboring Co layers in Au/Co multilayers are strongly ferromagnetically coupled when $t_{\text{Au}} < 15 \text{ \AA}$, and magnetization direction nearly lies in the film plane, the distribution of the magnetization may be reduced; hence, the ratio σ_r/σ_s is comparatively large in parallel geometry. Similarly, it is difficult to reserve the magnetic domains in magnetic reversal process when $t_{\text{Au}} < 15 \text{ \AA}$; moreover, FMR measurements have shown that the in-plane anisotropy field increases with the decrease of the Au layer thickness for $t_{\text{Co}} = 10 \text{ \AA}$. Hence, the coercivity in parallel geometry is large. On the other hand, when $t_{\text{Au}} > 15 \text{ \AA}$, the exchange coupling between the neighboring Co layer is weak, and the magnetic domains in the neighboring Co layers are decoupled; thus σ_r/σ_s and H_c change only slightly when $t_{\text{Au}} > 15 \text{ \AA}$.

Examples of FMR spectra for Au/Co multilayers are shown in Fig. 5. It is seen that the FMR spectrum consists of a main mode and a higher-field mode in parallel geometry ($\phi_H = 0$). With the increase of the angle (Φ_H) between H and the film plane, the resonance fields for both modes increase. At a given value of Φ_H , the two

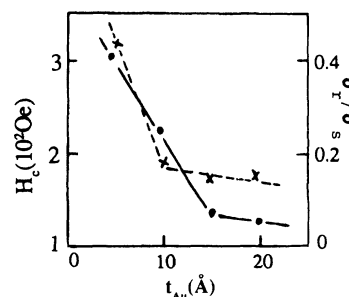


FIG. 4. The dependence of σ_r/σ_s (\times) and H_c (\bullet) on a Au layer thickness t_{Au} for Au/Co multilayers with a fixed Co layer thickness of 10 \AA in parallel geometry.

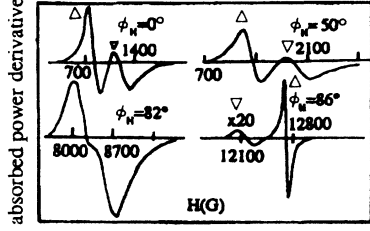


FIG. 5. The dependence of the absorbed power field derivative on the applied static field H at four orientations ϕ_H for a $[\text{Au}(20 \text{ \AA})/\text{Co}(30 \text{ \AA})]_{25}$ multilayer. At $\phi_H = 0, 50^\circ, 86^\circ$, the two modes are well identified; at $\phi_H = 82^\circ$, the two modes are not resolved. Δ , internal Co mode; ∇ , outermost Co mode.

modes cross each other. When Φ_H further increases, the two modes separate again, and the resonance field for the main mode is larger than that for the higher-field mode. At the end of Ref. 6, the higher-field mode was observed in nearly perpendicular geometry, but it was not systematically analyzed.

In Fig. 6, the dependence of both resonance fields and the difference of resonance fields on the thickness of the Co layer is shown. It is seen that both the resonance fields of the two modes and their difference decrease with increasing the thickness of the Co layer, indicating that the higher-field mode seems not to be the surface Damon-Eschbach (DE) mode observed in thick magnetic films and multilayers.¹¹

From the FMR spectra in Fig. 5, it is seen that the relative strength of the higher-field mode to the main mode is much larger in parallel geometry than in nearly perpendicular geometry, and that linewidth of the higher-field mode is broader than that of the main mode in both parallel and perpendicular geometry. Therefore, we suggest that the two modes are a result of difference of two surface Co layers from the internal Co layers inside the Au/Co multilayers. Since the properties of the thin internal Co layers are clearly influenced by their proximity to neighbors, producing higher effective magnetization and narrow FMR linewidth (the main mode); the outermost Co layers, similar to that in a Au/Co/Au sandwich,⁶ form the higher-field mode with low magneti-

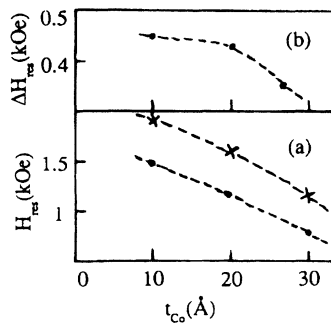


FIG. 6. (a) The dependence of the resonance field H_{res} of the main (\bullet) and the higher field (\times) modes on the Co layer thickness t_{Co} for Au/Co multilayers with a fixed Au layer thickness of 20 \AA in parallel geometry. (b) $\Delta H_{\text{res}} = H_{\text{res}}$ (higher-field mode) $- H_{\text{res}}$ (main mode).

zation and broad FMR linewidth. The intensities of the bulk relative to the surface are reduced by skin depth effects.

For uniform precession of the magnetization of the Co layer, the resonance field H_{res} is expressed as follows:⁵

$$(\omega/\gamma)^2 = [H_{\text{res}} \cos(\phi_H - \phi) + H_A \cos 2\phi + H_{2A} (3 \sin^2 \phi \cos^2 \phi - \sin^4 \phi)] \times [H_{\text{res}} \cos(\phi_H - \phi) - H_a \sin^2 \phi - H_{2A} \sin^4 \phi], \quad (2)$$

where ϕ is the static equilibrium position of magnetization, and H_A and H_{2A} are the internal field and the second-order anisotropy field, respectively.

By fitting the experimental data of the two modes with Eq. (2), similar to that of the Au/Co/Au sandwich,⁵ the fitted result is good, indicating that the above theoretical model can well explain the dependence of resonance field H_{res} on the orientation of the applied dc magnetic field ϕ_H for both modes. Some of the fitted H_A and H_{2A} values are tabulated in Table I.

For both modes, the effective internal field H_A is expressed as follows:

$$H_A = 4\pi M - H_{1A} - H_{2A}, \quad (3)$$

where M is the magnetization of the Co layer, and H_{1A} is the first-order anisotropy field. If the interface anisotropy (K_s) essentially enhances the first-order anisotropy,⁵ we can get from Eqs. (1) and (3)

$$H_A + H_{2A} = (4\pi M_A - H_v) - 2H_s/t_{\text{Co}}, \quad (4)$$

where H_v and H_s are the effective volume and interface anisotropy field, $H_{v,s} = 2K_{v,s}/M$, respectively. If $H_A + H_{2A}$ is plotted as a function of $1/t_{\text{Co}}$ for the resonance mode of the outermost Co layers (within a fixed Au layer thickness of 20 \AA , see Table I) at room temperature, a linear variation is obtained as displayed in Fig. 7, showing that Eq. (4) describes our data reasonably well. From the slope of the line and its intersection with the axis, $4\pi M - H_v = 10.6 \text{ KOe}$, and $H_s = 3.5 \times 10^{-4} \text{ Oe}$ are obtained. If $M = 1.25 \text{ KG}$ [the magnetization of the Au (20 $\text{\AA})/\text{Co}(10 \text{ \AA})]_{27}$ multilayer) is assumed, $K_v = 3.19 \times 10^6 \text{ erg/cm}^3$ and $K_s = 0.22 \text{ erg/cm}^2$ are obtained. With respect to that revealed by magnetic measurements, the K_v value obtained from FMR is smaller, but the K_s value is slightly larger. Moreover, in Fig. 7, $H_A + H_{2A}$ vs

TABLE I. The values of the internal field H_A and the second-order anisotropy field H_{2A} (units: KOe) for the internal Co mode (second and third columns) and the outermost Co mode (fourth and fifth columns) for three representative Au/Co multilayers.

Sample	H_A	H_{2A}	H'_A	H'_{2A}
$[\text{Au}(20 \text{ \AA})/\text{Co}(10 \text{ \AA})]_{27}$	6.08	-0.15	3.90	-0.30
$[\text{Au}(20 \text{ \AA})/\text{Co}(20 \text{ \AA})]_{24}$	8.25	0.28	6.20	0.84
$[\text{Au}(20 \text{ \AA})/\text{Co}(30 \text{ \AA})]_{25}$	12.59	0	8.25	0

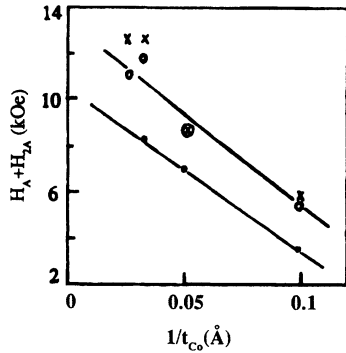


FIG. 7. $H_A + H_{2A}$ as a function of $1/t_{Co}$ for the outermost Co mode (●) with a fixed Au layer thickness of 20 Å and for the main mode (× for $t_{Au} = 20$ Å ○ for $t_{Au} = 30$ Å).

$1/t_{Co}$ for the main mode (the internal Co mode) is also plotted for Au/Co multilayers with the fixed $t_{Au} = 20$ and 30 Å, respectively. For $t_{Au} = 30$ Å, the neighboring Co layers are completely decoupled; hence, from Fig. 7, it

can be seen that Eq. (4) well describes its experimental data. From the fitting for the main mode of $t_{Au} = 30$ Å, the interface anisotropy field $H_s = 3.9 \times 10^{-4}$ Oe is obtained. This H_s value is in agreement with that obtained from the outermost Co mode.

CONCLUSION

In summary, we have systematically studied the magnetic properties of the evaporated Au/Co multilayers by magnetic measurements and ferromagnetic resonance. A mode with a lower internal anisotropy field, H_A , compared to the strongest mode, has been observed, and is attributed to the resonance of the outermost Co layers. Interface anisotropy has been obtained from magnetic measurements and FMR spectra. Furthermore, the strong dependence of σ_r/σ_s and H_c on the Au layer thickness may be understood as the effect of interlayer magnetic coupling.

- ¹J. Ferre, G. Penissard, C. Marliere, D. Renard, P. Beauvillain, and J. P. R. Renard, *Appl. Phys. Lett.* **56**, 1588 (1990).
²F. J. A. den Broeder, D. Kuiper, A. P. Vande Mosslaer, and W. Hoving, *Phys. Rev. Lett.* **60**, 2769 (1988).
³P. Gruberg, J. Barnas, F. Saurenbach, J. A. Fuss, A. Wolf, and M. Vohl, *J. Magn. Magn. Mater.* **93**, 58 (1991).
⁴S. S. P. Parkin, R. Bhadra, and K. P. Roche, *Phys. Rev. Lett.* **66**, 2152 (1991).
⁵C. Chappert, K. Le. Dang, P. Beauvillain, H. Hurdequint, and D. Renard, *Phys. Rev. B* **34**, 3192 (1986).

- ⁶H. Hurdequint and M. Malouche, *J. Magn. Magn. Mater.* **93**, 276 (1991).
⁷S. W. Mcknight and C. Vittoria, *Phys. Rev. B* **36**, 8574 (1987).
⁸C. H. Lee, H. He, F. Lamedas, W. Vavra, C. Uher, and R. Clarke, *Phys. Rev. Lett.* **62**, 653 (1989).
⁹C. Gao and M. J. O' Shea, *J. App. Phys.* **69**, 5304 (1991).
¹⁰P. Bruno, *J. Phys. F* **18**, 1291 (1988).
¹¹R. E. Camley, T. S. Rahman, and D. L. Mills, *Phys. Rev. B* **27**, 261 (1983).